ELSEVIER
SAUNDERS

Magn Reson Imaging Clin N Am
12 (2004) 281–299

MAGNETIC
RESONANCE
IMAGING CLINICS
of North America

MR imaging findings in ulnar-sided wrist impaction syndromes

Luis Cerezal, MD[a,*], Francisco del Piñal, MD, PhD[b], Faustino Abascal, MD[a]

[a]*Department of Radiology, Instituto Radiológico Cántabro, Clínica Mompía, Mompía, 39109 Cantabria, Spain*
[b]*Private Hand-Wrist and Plastic-Reconstructive Surgery and Hand Surgery Department, Mutua Montañesa, Calderón de la Barca 16-entlo, 39002-Santander, Spain*

Ulnar wrist constitutes a complex anatomic region that has evolved considerably in the last stages of phylogenic development. The fact that the distal radioulnar joint (DRUJ) and the triangular fibrocartilage (TFC) complex are such complicated structures is one of the features that separates the family of hominoidea, which humans belong to, from the lesser-developed animals [1,2].

The diagnosis and management of ulnar wrist disorders has historically been a diagnostic challenge for radiologists and hand surgeons. Widespread interest in the ulnar wrist and DRUJ during the past decades has resulted in a much clearer understanding of the anatomy, biomechanics, and pathologic conditions affecting this anatomic area, and as a result of this, great advances in the diagnostic and therapeutic abilities in patients with ulnar-sided wrist pain [1,3–6]. Ulnar wrist pain is a common and frequently disabling complaint that may be caused by a broad spectrum of osseous or soft-tissue disorders, including TFC complex tears, DRUJ arthritis and instability, lunotriquetral (LT) ligament disruption, Kienböck disease, pisotriquetral arthritis, extensor carpi ulnaris (ECU) lesions [7], and ulnar-sided wrist impaction syndromes [8].

Ulnar-sided wrist impaction syndromes are a common source of ulnar pain and limitation of motion that result from repetitive or acute forced impingement between the distal ulna and ulnar carpus or distal radius and surrounding soft tissues, resulting in bone or soft-tissue lesions [8].

In an adequate clinical setting, conventional radiographic findings of anatomical variants or pathologic conditions of the ulnar wrist can suggest the diagnosis of a given ulnar-sided impaction syndrome. However, diagnosis remains difficult and often delayed because symptoms and clinical findings are usually nonspecific and similar among the different pathologic conditions in the ulnar-sided wrist; moreover, significant disease and incapacitating pain may be present despite minimal evidence at conventional radiography [8].

This article reviews the concept of ulnar variance; the pathophysiology, clinical diagnosis, conventional radiographic and MR imaging findings; and treatment of different ulnar-sided wrist impaction syndromes. Also discussed is the usefulness of MR imaging in the preoperative evaluation of these entities.

Ulnar variance

Compressive loads across the wrist are borne principally by the distal radius but also are transmitted through the TFC complex to the ulnar head [5,6,9]. The distribution of the load is greatly influenced by the relative lengths of the distal articular surfaces of the ulna and the radius. This is referred to as ulnar variance or radioulnar index: neutral variance (both the same length), positive variance (ulna longer), and negative variance (ulna shorter) (Fig. 1) [10]. Eighty

* Corresponding author.
E-mail address: lcerezal@mundivia.es (L. Cerezal).

1064-9689/04/$ - see front matter
doi:10.1016/j.mric.2004.02.005

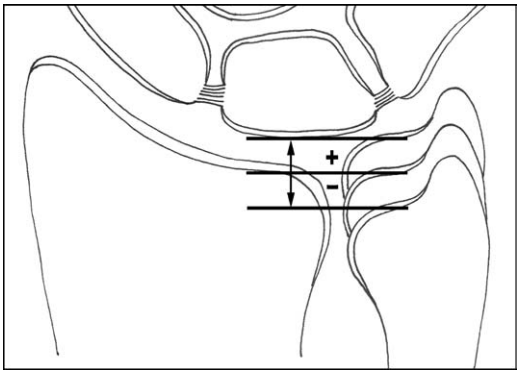

Fig. 1. Ulnar variance. The degree of variance is determined by projecting a line perpendicular from the carpal joint surface of the distal end of the radius toward the ulna and measuring the distance in millimeters between this line and the carpal surface of the ulna. Positive ulnar variance or ulna plus with the articular surface of the ulna projecting distal to the articular surface of the radius, distal variance with equal length of the distal articular surfaces of the radius and ulna, and negative variance or ulna minus with the distal edge of the ulna proximal to the distal articular surface of the radius.

percent of the compressive load across the wrist is transmitted through the radiocarpal articulation, and 20% is transmitted through the ulnocarpal articulation with a neutral ulnar variance. Small changes in ulnar variance can alter this force distribution markedly. A change of the ulnar variance of only 1 mm can change the mechanical load on the ulnocarpal joint by more than 25% (see references [5,6,9,11]).

Ulnar variance is not static; changes in forearm position and power grip continually alter it [12–15]. Full forearm pronation increases ulnar variance; full forearm supination decreases it. Ulnar variance also becomes more positive with power grip and returns to its original state with cessation of grip. Variance changes related to forearm rotation and grip may be as much as 2 to 3 mm [12–14]. Changes of this magnitude demonstrate the large load alterations across the ulnocarpal articulation during daily activities involving rotation of the forearm and grip.

It is obvious that a standard position for radiographs is necessary to predictably reproduce results for determining ulnar variance. The generally accepted standard is for a posteroanterior radiograph to be taken with the wrist in neutral forearm rotation, the elbow flexed 90 degrees and the shoulder abducted 90 degrees, which provides an image of the radioulnar length with the wrist unloaded [12–17]. Such a view may underestimate variance in wrists in which power grip and pronation result in significant proximal migration of the radius. Therefore preoperative ulnar variance should be measured using neutral rotation and pronated grip radiographs before selecting treatment for causes of ulnar wrist pain that are affected by radioulnar length [13,14]. Although MR imaging can estimate the degree of ulnar variance, direct ulnar variance measurements from standard wrist MR images are not appropriate. MR imaging usually fails to duplicate the specific position for determining ulnar variance, and the radiologist must exercise caution in describing subtle ulnar variance on MR images of the wrist [8,18].

Classification

Ulnar-sided wrist impaction syndromes can be divided into five main categories: (1) ulnar impaction syndrome; (2) ulnar impingement syndrome; (3) ulnar styloid impaction syndrome; (4) hamatolunate impaction syndrome; and (5) combined ulnar and ulnar styloid impaction syndrome.

Ulnar impaction syndrome

Ulnar impaction syndrome, also known as ulnar abutment or ulnocarpal impaction, is a degenerative condition characterized by ulnar wrist pain, swelling, and limitation of motion related to excessive load bearing across the ulnar aspect of the wrist [16,19–21]. Chronic impaction between the ulnar head and the TFC complex and ulnar carpus results in a continuum of pathologic changes: degenerative tear of the TFC; chondromalacia of the lunate bone, triquetral bone, and distal ulnar head; instability or tear of the LT ligament (Fig. 2); and, finally, osteoarthritis of the DRUJ and ulnocarpal joint [16,19–21].

Palmer [22] designed a classification system for TFC complex lesions based on mechanism, location, and involved structures. This classification system is helpful in determining the mechanism of injury and directing clinical management. It divides lesions into two classes. Class I (traumatic) lesions are subclassified according to the site of TFC complex involvement. Class II (degenerative) lesions demonstrate the entire spectrum of findings in ulnar impaction syndrome and are subclassified according to the degree of

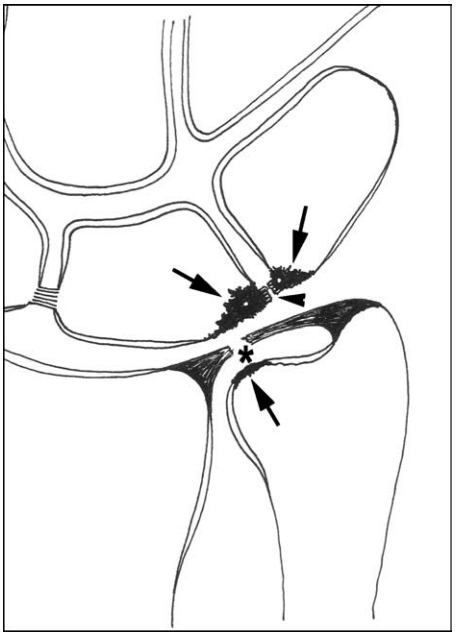

Fig. 2. Diagram illustrates the full spectrum of pathologic conditions in ulnar impaction syndrome, including chondromalacia of the ulnar head, the ulnar side of the lunate bone, and the radial side of the triquetral bone (*arrows*); central perforation of the triangular fibrocartilage (TFC) (*small arrowhead*); and lunotriquetral (LT) ligament tear (*asterisk*).

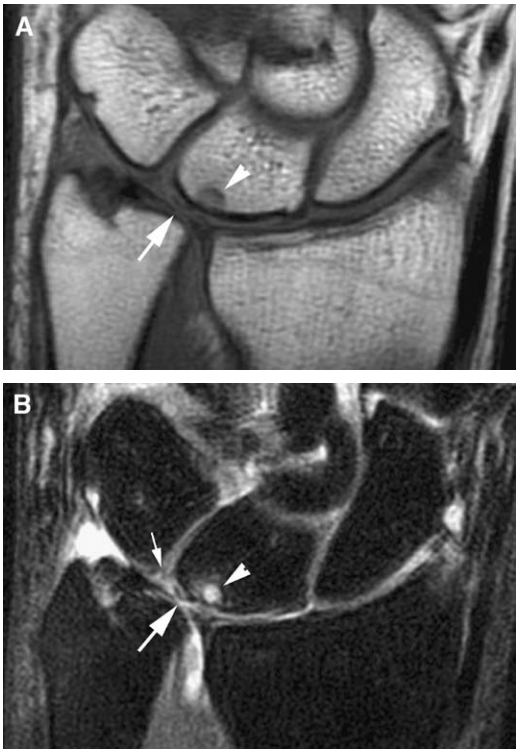

Fig. 3. Ulnar impaction syndrome in a 36-year-old man with positive ulnar variance and insidious onset of ulnar-sided wrist pain (Palmer class IID lesion). Coronal T1-weighted (*A*) and coronal fat-suppressed T2-weighted (*B*) MR images show positive ulnar variance, central perforation of the triangular fibrocartilage (TFC) (*arrow*), chondromalacia of the lunate bone with secondary subchondral changes (*arrowheads*), and partial lunotriquetral (LT) ligament tear (*small arrow*). An arthroscopic "wafer" procedure and debridement of the LT was performed with excellent results.

involvement of structures on the ulnar side of the wrist, highlighting the progressive nature of these injuries. Class IIA injuries represent TFC complex wear. Class IIB injuries include TFC complex wear with associated lunate or ulnar chondromalacia. Class IIC injuries represent a TFC complex perforation in association with lunate or ulnar chondromalacia. Class IID lesions include a TFC complex perforation, lunate or ulnar chondromalacia, and LT ligament perforation (Fig. 3). Class IIE injuries include a TFC complex perforation, lunate or ulnar chondromalacia, LT ligament perforation, and additional ulnocarpal arthritis.

The pathologic changes that appear in ulnar impaction syndrome most commonly occur with positive ulnar variance but can occasionally occur with neutral or negative ulnar variance [19,23,24]. The most common predisposing factors include congenital positive ulnar variance, malunion of the distal radius (Fig. 4), premature physeal closure of the distal radius, Essex-Lopresti fracture, and previous surgical resection of the radial head [19]. All of these predisposing factors result in a fixed increase in underlying ulnar loading associated with relative lengthening of the ulna or increased dorsal tilt of the distal radius. The biomechanical and anatomical data available therefore suggest a direct causal relationship between increased force distribution across the ulnar aspect of the wrist joint and the spectrum of pathologic changes known as the ulnar impaction syndrome [19,21].

In the absence of obvious structural abnormalities, ulnar impaction syndrome may result from daily activities that cause excessive intermittent loading of the ulnar carpus. It also has been shown that asymptomatic changes in ulnar impaction syndrome develop over time, so that this condition may be present even if symptoms are not evident [19,21,25].

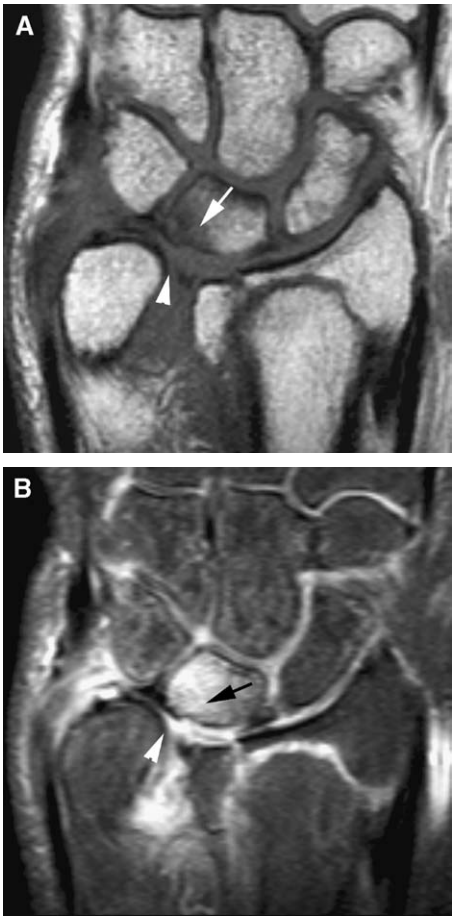

Fig. 4. Ulnar impaction syndrome secondary to malunited distal radial fracture in a 32-year-old man. Coronal T1-weighted (*A*) and coronal fat-suppressed T2-weighted (*B*) MR images reveal central triangular fibrocartilage (TFC) tear (*arrowheads*), chondromalacia, cortical irregularity, and subchondral bone marrow edema in the ulnar aspect of the lunate bone (*arrows*). Reconstruction with an opening-wedge osteotomy and fixation with an oblique T-plate restored near-anatomic relationships at the radiocarpal joint and the distal radioulnar joint (DRUJ).

The clinical manifestation of ulnar impaction syndrome generally consists of chronic or subacute ulnar wrist pain, often exacerbated by activity and relieved by rest. Anything that causes a relative increase in ulnar variance (eg, firm grip, pronation, ulnar deviation of the wrist) evokes increased symptoms [19,21].

Physical examination reveals swelling and tenderness that is usually localized to the region of the TFC complex and LT joint [26]. Limitation of forearm rotation and wrist motion usually is present.

Radiographic findings in ulnar impaction syndrome include positive ulnar variance and, less frequently, neutral or negative variance [19,23]. Pronation grip radiographs are useful in determining the increase in ulnar variance and the impaction between ulnar carpus and the dome of the ulnar head [19,23]. Underlying abnormalities, including malunion of a distal radial fracture with residual radial shortening and abnormal dorsal tilt, may be present. Premature physeal arrest of the distal radius or previous Essex-Lopresti fracture or resection of the radial head also may be evident on conventional radiographs [19]. Secondary changes in the ulnar carpus include subchondral sclerosis and cystic changes in the ulnar head, ulnar aspect of the proximal lunate bone, and proximal radial aspect of the triquetral bone [19,20]. Although the radiographic changes may be striking, the features of ulnar impaction syndrome may be subtle in its early and late stages [8]. Recognition of the geographic nature of the abnormalities affecting the articular surfaces of the ulna, lunate bone, and triquetral bone is paramount for making the correct diagnosis [16,19,21].

In the setting of negative or questionable negative conventional radiographs and a strong clinical suspicion for ulnar impaction, MR imaging is helpful in detecting radiologically occult lesions [19,20]. Softening, fibrillation, or partial-thickness defects of articular cartilage in the wrist are detected inconsistently by MR imaging; however, the accuracy of MR imaging tends to be more favorable for high-grade or large cartilage defects. Indirect or secondary signs of chondromalacia manifested with subchondral bone marrow edema (see Fig. 4), particularly conspicuous on fat-suppressed T2-weighted and STIR images, and synovitis are frequent findings in ulnar impaction syndrome [19–21]. Bone marrow edema can even be seen in patients without cartilaginous degeneration revealed at arthroscopy, indicating that it is also a sensitive sign of ulnar impaction.

Progression of the syndrome results in sclerotic changes, which appear as areas of low signal intensity on T1- and T2-weighted images, and subchondral cysts, which appear as well-defined areas of low signal intensity on T1 and high signal intensity on T2-weighted images (see Fig. 3). These changes usually are appreciated much earlier in MR images than in conventional radiographs.

In patients with radiographic evidence of ulnar impaction syndrome, MR imaging and MR arthrography may be necessary to demonstrate the integrity of the TFC and LT ligament.

Degenerative changes of the TFC, usually histologic mucinous or myxoid degeneration, are best depicted on T2*-weighted images, and appear as contours irregularities, thinning, or attenuation with associated regions of increased signal intensity. Degeneration is common in the thinner central portion of the TFC. TFC tears, demonstrated by discontinuity or fragmentation, are most commonly located near or adjacent to the radial attachment. A well-defined fluid signal crossing the TFC on T2-weighted images constitutes a highly specific indicator of a perforation (see Fig. 3B) [27–30]. MR imaging is particularly helpful in the assessment of degenerative changes and partial tears involving the proximal ulnar dome aspect of the TFC that are arthroscopically occult.

Because the incidence of asymptomatic perforations increases with increasing age, the clinical significance of an MR imaging determined TFC lesion must always be carefully correlated with the patient clinical presentation.

The LT ligament is consistently visible with MR imaging when it is present. This ligament is triangular in 63% of patients and linear in 37% [31]. The signal intensity is homogeneous and low in intensity in 75% but a linear brighter signal traverses part or all of the LT ligament in 25%. This linear signal is distinguishable from a tear because it is not as bright as fluid signal [27,31]. Disruption of the ligament is shown on T2*-weighted or fat-suppressed T2-weighted images as either complete ligamentous disruption or as a discrete area of linear bright signal intensity in a partial or complete tear (see Fig. 3B). In complete tears, synovial fluid communication between the radiocarpal and midcarpal compartments may be identified. Unlike ligament dissociations, perforations of the LT ligament are not associated with osseous widening of the LT articulation, which makes more difficult the diagnosis, especially in the absence of adjacent fluid [31]. Small membranous perforations may exist in the presence of intact dorsal and volar portions of the LT ligament. Most degenerative perforations occur in the thin membranous portion of the LT ligament and are difficult to appreciate on MR images [31].

There is a wide range of reported sensitivities (40% to 100%) and specificities (33% to 100%) for the diagnosis of LT ligament perforations using MR imaging. MR imaging is superior to conventional arthrography, allowing identification of the size, morphology, and location of an LT ligament tear. This information is important because communication, across a pinhole or small perforation or deficiency of the thin membranous portion of the ligament, may not be significant in the presence of grossly intact dorsal and volar ligaments [31].

MR arthrography may be necessary in selected cases to clarify the exact stage of ulnar impaction in the preoperative evaluation. This technique is especially useful in determining the perforation or not of the TFC (Palmer class IIB versus IIC), in determining the status of the ulnocarpal ligaments (Fig. 5), and the LT ligament (Palmer class IIC versus IID).

The differential diagnosis must include intraosseous ganglia, true cysts, vascular grooves, and Kienböck disease [8,20,21]. The distribution of radiographic changes within the lunate bone is the key to distinguishing these conditions from ulnar impaction. Intraosseous ganglia and true cysts appear on conventional radiographs as a radial-sided area of hyperlucency that communicates with the scapholunate joint space or a hyperlucent area within the distal ulnar aspect of the lunate bone that communicates with the LT joint space. Intraosseous ganglia and true cysts demonstrate low signal intensity on T1-weighted MR images and high signal intensity on T2-weighted images, similar to water. Differentiation is aided by a lack of clinical findings, sharper margins seen on radiographs, and a lack of changes in signal intensity in the triquetral bone or ulnar head [20,21]. A vascular groove usually appears as a central proximal radiolucent defect that communicates with the radiolunate joint space [21]. The signal intensity pattern in Kienböck disease may mimic that in ulnar impaction syndrome; however, Kienböck disease lesions are more diffuse or affect the radial half of the lunate bone compared with involvement of only the ulnar aspect in ulnar impaction syndrome. Furthermore, the triquetral bone and the ulnar head are not affected in Kienböck disease [20,21].

Briefly, there are three types of procedures that can be used when dealing with symptomatic ulnar impaction: wafer procedure, arthroscopic wafer, and formal ulnar shortening (see references [4,19,32,33]). They all aim to recede the dome of the head of the ulna [32]. In the wafer procedure, the distalmost 2 to 3 mm of the dome of the ulnar

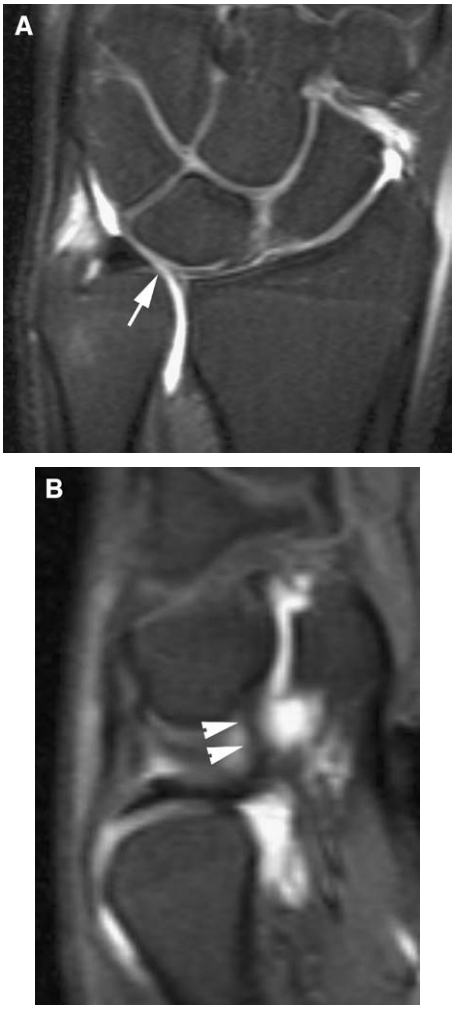

Fig. 5. Ulnar impaction syndrome in a 34-year-old man with chronic ulnar-sided wrist pain. Fat-suppressed T1-weighted coronal (*A*) and sagittal (*B*) arthrographic MR images demonstrate central triangular fibrocartilage (TFC) perforation with fluid communication between the radiocarpal and distal radioulnar compartments (*arrow in A*) and intact lunotriquetral (LT) ligament (*arrowheads in B*). An arthroscopic wafer procedure was performed with good results.

head are resected by a limited approach centered on the DRUJ. This can be performed by arthroscopic instrumentation (arthoscopic wafer) [33]. In the ulna shortening, the distal shaft of the ulna is approached dorsolaterally and the desired amount of ulna is removed, as a slice, followed by rigid fixation [4,19].

Which method to use depends on multiple considerations, including, but not limited to, the amount of ulnar variance, the Palmer type, the shape of the sigmoid fossa and ulnar seat, the presence of concomitant LT instability, and the surgeon's skill level [34–37]. The morphology of the sigmoid notch should be carefully assessed with MR imaging and classified according the classification described by Tolat and subsequent subclassification by Deshmukh [36,37]. A Tolat type I DRUJ has a sigmoid notch and ulnar seat angle roughly parallel to each other and to the long axis of the ulna, type II has a joint surface that is oblique and pointing toward the distal part of the ulna, and type III has a reverse oblique orientation. If a Tolat type III sigmoid notch is present, ulnar shortening will produce joint incongruity with impingement of the ulnar head on the proximal edge of the notch.

Palmer class IIA and IIB lesions (no TFC perforation) are managed with an open wafer procedure [24,32,38]. When the TFC is already perforated (Palmer class IIC and IID lesions), the head of the ulna can be burred down with the help of arthroscopic instrumentation (arthroscopic wafer procedure) [33]. This procedure is minimally invasive, highly effective, and allows rapid return to normal activities. Some authors currently consider it optimal to perforate the TFC in class IIA and IIB lesions and then perform an arthroscopic wafer procedure, as one would in IIC and IID lesions [33]. More recently, Dailey and Palmer [4] further differentiated two subtypes of type IID (LT perforation): one with only perforation of the ligament, and a second one with associated instability of the LT joint. In the former, arthroscopic debridement would be enough, but in the latter, associated ulnar shortening osteotomy is recommended as this will tighten the ulnolunate and ulnotriquetral ligament and stabilize minor degrees of LT instability. If this is not enough, and instability persists, as evidenced by artroscopy, direct treatment of the LT instability is required as the patient will remain symptomatic if this instability is not dealt with, but this beyond the focus of this article [39]. Class IIE lesions are managed with salvage procedures, such as complete or partial ulnar head resection (Darrach and similar procedures) or arthrodesis of the DRUJ with distal ulnar pseudoarthrosis (Sauvé-Kapandji procedure) [4]. Unfortunately, none of these procedures is ideal because they all produce convergent instability (discussed later).

There are several exceptions to this "cookbook" approach, among the most important are

neither the wafer open or arthroscopic is recommended when the ulna is positive more than 3 or 4 mm, in those cases formal ulnar shortening osteotomy is a better choice [32,33]. Conversely, the latter is not indicated when dealing with Tolat type III DRUJ [36] as this will cause concentration of a high load of compressive and shearing forces in a small spot and hence a form of impingement [35]. Similarly, the less well known Deshmukh concentric radioulnar shapes also will promote early degeneration if the ulna head is shortened for similar reasons. Ulnar impaction secondary to an Essex-Lopresti fracture-dislocation deserves separate consideration too, because successful treatment is not possible in the chronic setting [40,41]. Ulnar shortening in particular is doomed to failure because the ruptured interosseous membrane allows the radial column to recede until the proximal radial metaphysis impacts against the capitellum. Thus, it is vital to consider the feasibility of an Essex-Lopresti injury in any impaction fracture of the radial head in the acute setting. This will allow appropriate management of the full injury and not just of the radial head fracture.

Ulnar impingement syndrome

The terms "ulnar impingement" and "ulnar impaction" often are used interchangeably; however, these entities are not only distinct but also mutually exclusive. Ulnar impingement syndrome is painful condition caused by a shortened distal ulna that impinges on the distal radius proximal to the sigmoid notch [21,42,43].

A markedly shortened distal ulna results most frequently from any of the surgical procedures that involve resection of the distal ulna secondary to prior wrist trauma, rheumatoid arthritis, or correction of Madelung deformity (Fig. 6A). Ulna head resection (Bowers), fusion or resection of the distal ulna (Sauvé-Kapandji), hemiresection interposition arthroplasty (Watson), and several modifications of these procedures are some of the surgical techniques that may be complicated with the development of ulnar impingement [21,42,43]. Less commonly, ulnar impingement may be present in de novo cases of negative ulnar variance or premature fusion of the distal ulna secondary to prior trauma (Fig. 6B) [21,42,43].

When the distal ulna is shortened for whatever reason, the contraction of the extensor pollicis brevis, abductor pollicis longus, and pronator quadratus muscles and the effect of the interosseous membrane with the loss of the buttress effect of the radioulnar joint cause approximation of the lower ends of the radius and ulna. This is known as radioulnar convergence and is rarely symptomatic, in contrast to ulnar impingement syndrome, in which distal radioulnar contact is evident and causes pain (see Fig. 6A) [42,43].

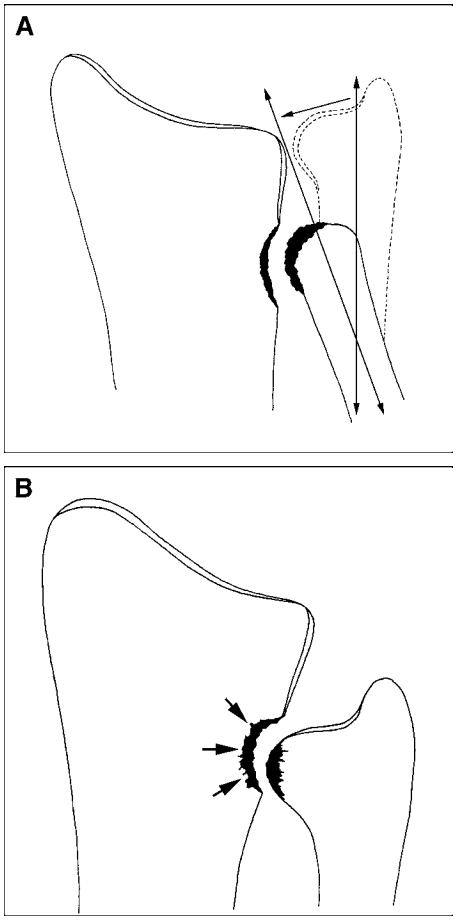

Fig. 6. Diagrams illustrate the cardinal features of ulnar impingement. (*A*) Ulnar impingement syndrome secondary to distal ulnar resection: a shortened ulna proximal to the sigmoid notch, scalloping of the distal radius, and radioulnar convergence (*arrow*). (*B*) Ulnar impingement secondary to significant negative ulnar variance or premature fusion of the distal ulna. Note the scalloping of the distal radius proximal to the sigmoid notch (*arrows*).

The clinical manifestation of ulnar impingement syndrome can be similar to that of ulnar impaction syndrome. Typically the patients experience pain on pronation and supination of the forearm and weakness on lifting even light objects.

Compression of the DRUJ on forearm rotation increases the symptoms or produces grating in affected patients and is useful in identifying incongruity of the DRUJ. The clinical diagnosis is commonly missed because it is not specifically sought [42,43].

Ulnar impingement can produce erosive and proliferative cortical changes along the ulnar margin of the distal radius proximal to the sigmoid notch level that appear as scalloping and bone hypertrophy on conventional radiographs (Fig. 7A) [21,43,44]. By the time such changes are seen, the condition has been present for many years. The stress-loaded radiologic view described by Lees and Scheker [44] will confirm the diagnosis before erosive changes are visible showing the radioulnar convergence. This radiologic projection is performed by asking the patient maximally gripping a cylindrical object 2 cm in diameter with the shoulder adducted, the elbow flexed to 90 degrees, and the forearm in the position of neutral rotation. The radiograph is then taken with the beam aligned in the coronal plane with respect to the anatomical position [44].

MR imaging is helpful in confirming the diagnosis before erosive changes are visible in the conventional radiographs, showing subtle sclerosis and bone edema at the corresponding level of the radius and on the distal ulna [8]. In advanced stages, scalloping and sclerosis along the ulnar margin of the distal radius cephalad to the sigmoid notch, sclerosis in the ulnar seat and bony spurs or osteophytes in both margins are clearly visualized on MR images (Figs. 7B and 8).

Although convergence is common after the Darrach procedure and similar procedures, symptomatic ulnar impingement is rare—which is fortunate, because fully successful treatment does not yet exist. Aggressive ulnar shortening has been proposed [45], but the procedure has not yet stood the test of time. Scheker (L.R. Scheker, unpublished data, 2001) considers that further excision of the ulna is irrational and will result is further proximal impingement.

Attempts of contending ulnar shaft convergence and hypermobility after Darrach operation by tenodesis with the ECU [46], alone or in combination with the flexor carpi ulnaris [47], has not been rewarding in the clinical practice. Interposition of different materials, such as tendon, fascia, or allograft, may be successful in the middle term and for low-demand individuals [48].

Perhaps the definitive answer lies in ulnar head prostheses [49–52], which presently are not appropriate for patients who would place high demands on them. The approach is totally different when convergence is the result of a severely shortened ulna caused by a growing defect because distraction lengthening of the ulna can restore the normal anatomy [53]. With the application of Scheker's principles for treatment of early DRUJ osteoarthritis [54], less marked ulnar shortness might benefit from radial shortening performed in an attempt to change the

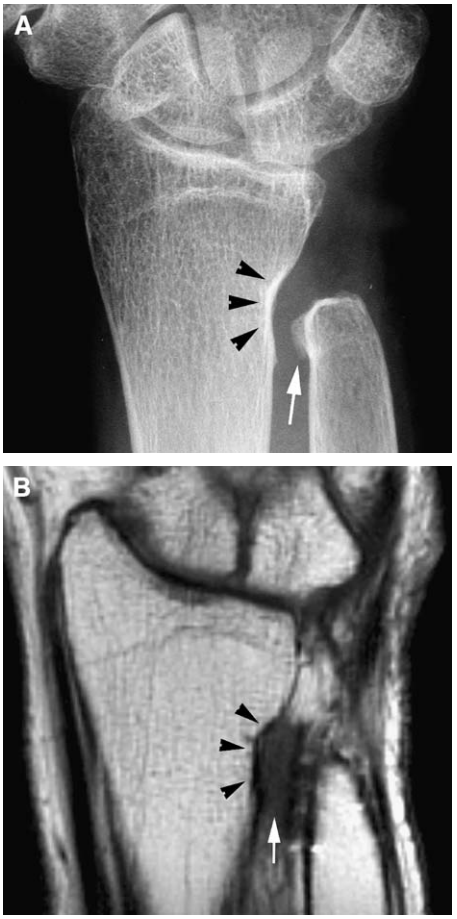

Fig. 7. Ulnar impingement in a 68-year-old man. The patient referred distal forearm pain since undergoing the Darrach procedure 6 years earlier. Posteroanterior radiograph (*A*) shows extensive distal ulnar excision, focal remodeling and sclerosis of the distal radius (*arrowheads*), and proliferative changes in the distal ulnar stump (*arrow*). Coronal T1-weighted image (*B*) reveals focal remodeling and sclerosis at the distal radius proximal to the sigmoid notch (*arrowheads*). Note soft-tissue thickening interposed between distal radius and ulnar stump (*arrow*).

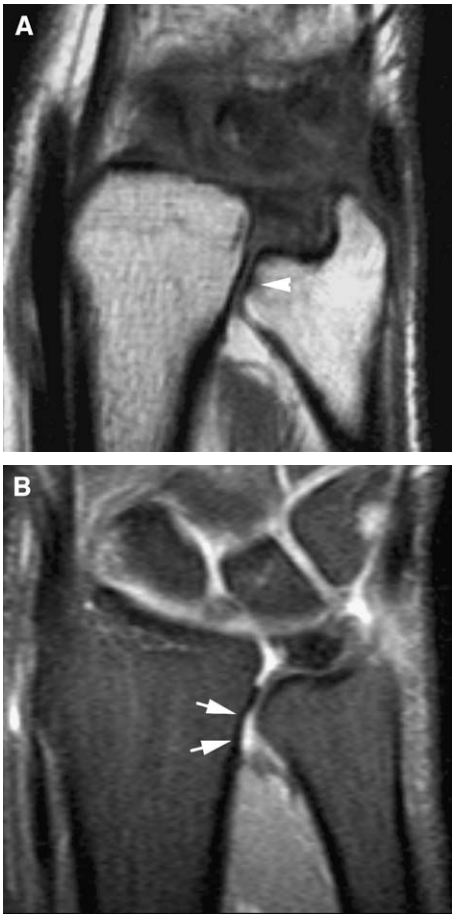

Fig. 8. Ulnar impingement in a 23-year-old man with chronic ulnar wrist pain and limitation of the forearm motion. Coronal T1-weighted (*A*) and coronal fat-suppressed T2-weighted (*B*) MR images demonstrate negative ulnar variance, subtle radial remodeling (*arrows in B*), and chondromalacia in the ulnar seat (*arrowhead*).

contact area between the ulnar head and the sigmoid notch. Finally, in the setting of ulnar shortness, consideration should be given to generalized wrist disorders, such as minor forms of ulnar club hand, because isolated lengthening of the ulna will not be successful in these cases as the surgeon has to act on the radius frontal malalignment too [55].

Ulnar styloid impaction syndrome

Ulnar styloid (US) impaction syndrome is an underrecognized etiology of ulnar wrist pain caused by impaction between the US and the triquetrum bone and the surrounding soft tissues

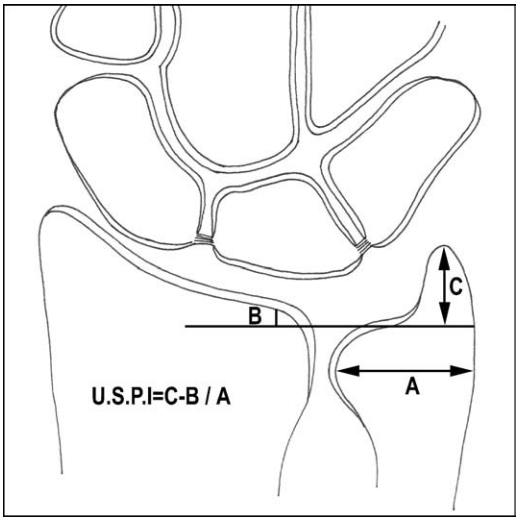

Fig. 9. Diagram illustrates the ulnar styloid (US) architecture measurements including US length and width, and the US process index (USPI). USPI is calculated by subtracting the degree of ulnar variance (B) from the length of the US process (C) and dividing the difference by the transverse diameter of the ulnar head (A). The USPI has a normal range of 0.21 ± 0.07.

[8,56]. This group of pathologic entities more commonly develop in wrists with negative ulnar variance and result from repetitive or acute forced ulnar deviation and dorsal flexion of the wrist [8,56,57].

Ulnar wrist has evolved considerably in the last stages of phylogenic development. One possible consequence of such a phylogenically rapid change is the frequent presence of anatomic variations, including supernumerary ossicles and morphological variations of the US [1,58,59]. The US process is a continuation of the prominent subcutaneous ridge of the shaft of the ulna, which projects distally toward the triquetral bone for a variable distance (3 to 6 mm) and with medial angulation exceeding 15 degrees [58,60]. Garcia-Elias [61] has developed a method of assessing the relative size of the US called the US process index (USPI) (Fig. 9). An excessively long US has a USPI greater than 0.21 ± 0.07 or an overall length greater than 6 mm [61].

US impaction syndrome may occur secondary to morphological variations (elongated, radially deviated, or enlarged US process) or pathological conditions (nonunion, malunion, or hypertrophy) of the US process.

The authors (Luis Cerezal and Francisco del Piñal, unpublished data, 2002) have designed

a classification system for US impaction syndromes in four subtypes based in different morphological or pathologic conditions of the US implicated in the etiology of this clinical entity (Box 1) (Fig. 10).

An elongated US is the commonest variant implicated in the development of US impaction syndrome (Fig. 11) [56,60]. Another anatomic variant is a US process curved in the volar and radial directions, giving a "parrot-beaked" appearance, which reduces significantly the styloid-carpal distance (Fig. 12). A pathologic sequence of events has been postulated in patients with US impaction syndrome with long or radially deviated US [56]. One-time or repetitive impaction between the tip of the US process and the triquetral bone results in contusion, which leads to chondromalacia of the opposing articular surfaces, synovitis, and pain. If a single-event trauma is forceful enough, fracture of the dorsal triquetral bone (chip fracture) may occur [61,62]. Impaction over a long period of time can lead to LT instability [56].

Enlarged US can be an anatomical variant or secondary to malunion of avulsion fracture at the fovea of the ulna (Fig. 13) [63]. This US morphological variation reduces the ulnar joint space developing repetitive impaction between US and ulnar aspect of the lunate bone and radial aspect of the triquetral bone. TFC complex wear or perforation is frequently present.

US fractures occur commonly in association with distal radius fractures [2,64–66]. Symptomatic nonunions of the US are probably underrecognized or underreported in the literature. Two types of nonunion of the US have been classically described on an anatomic basis and their different treatment [66]. Type I is defined as a nonunion associated with a stable DRUJ. It affects only the tip of the styloid and the TFC complex remains intact, as its major attachments are at the base of the styloid. Type II is defined as a nonunion associated with subluxation of the DRUJ. It is the result of an avulsion of the ulnar attachment of the TFC complex (Palmer class IB lesion). Recent evidence points to this subdivision as being an oversimplification, because although severely displaced basilar fractures of the US are more commonly associated with DRUJ instability, "chip" fractures can also be associated with instability if there is a concomitant TFC injury [67,68].

Box 1. Classification of US impaction syndromes

1. US impaction syndrome secondary to elongated US.
2. US impaction syndrome secondary to radially deviated US (parrot-beaked).
3. US impaction syndrome secondary to enlarged US.
4. US impaction syndrome secondary to US nonunion.
   A. With a stable DRUJ. Nonunion of the US with intact TFC complex ulnar attachment.
   B. With DRUJ instability. Nonunion of the US with avulsion of the ulnar attachment of the TFC complex.

A nonunion of the US may become symptomatic for different reasons. The nonunited fragment may act as an irritative loose body or abut the carpus [69]. A malaligned fibrous nonunion may cause impingement of the ECU tendon sheath. The nonunion may also be symptomatic because of associated TFC complex perforation or as stated as a result of complete rupture of the ulnar attachments of the TFC complex and hence an unstable DRUJ (Fig. 14) [8,66].

The diagnosis of US impaction syndrome is based primarily on the patient's clinical history and physical examination, and is supported by radiographic evidence of morphological variations or pathological conditions of the US [56].

The US architecture measurements (US length, angle, and width) and ulnar variance should be recorded in the neutral PA view of the wrist [60]. In advanced stages, plain radiographs may reveal degenerative changes in the US and the triquetrum bone [56].

MR imaging is the most useful imaging method for detecting the osseous and soft tissue abnormalities present in this syndrome and ruling out other potential causes of chronic ulnar wrist pain [8].

In patients with US elongated or radially deviated, MR imaging may show chondromalacia on the tip of the US and proximal triquetrum bone. Secondary subchondral changes, including bone marrow edema, sclerosis, and cysts, in characteristic locations can be detected in MR imaging in patients without significant abnormalities in the routine plain films (see Figs. 11 and 12). The presence of synovitis and joint effusion in the ulnocarpal joint also is common.

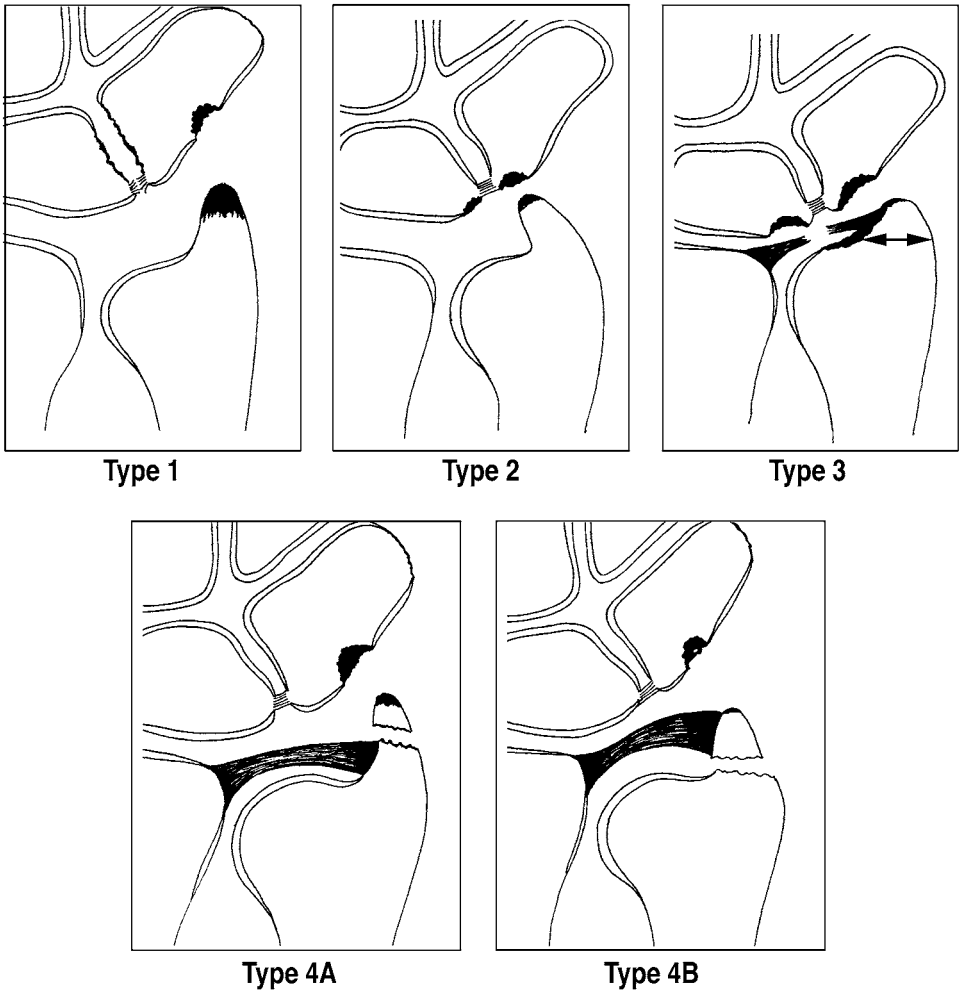

Fig. 10. Classification of ulnar styloid (US) impaction syndromes. Diagram illustrates the four different subtypes of US impaction syndrome and the pathologic conditions that characterize these entities.

In cases with enlarged US, the same findings can be seen in the ulnar aspect of the lunate, triquetrum, and US. MR imaging is helpful in the detection of degenerative fraying or tears of the TFC complex, which are frequent findings in these patients (see Fig. 13).

In patients with US impaction syndrome secondary to nonunion of the US, MR imaging is an excellent modality for visualizing the integrity of the TFC complex and its ulnar attachments, the presence of ununited bone fragments, and the associated chondromalacia and subchondral bone changes of the carpus (see Fig. 14). Tenosinovitis or tendinosis of the ECU secondary to irritative loose body can also be detected in MR imaging [8].

Resection of all but the two most proximal millimeters of the US process (so as not to interfere with the TFC complex insertion) is the treatment of choice in the US impaction syndrome secondary to elongated or parrot-beaked US [56].

Surgical treatment of the US impaction syndrome secondary to US nonunion should start by a diagnostic arthroscopy that allows allocating the condition to one of the above subtypes. If the TFC complex is lax, showing a positive trampoline sign [70], the ulna styloid (and with it the TFC complex) should be reinserted in the fovea and appropriately fixed by a limited incision in the ulnar aspect of the wrist [66]. If no TFC complex loosening is appreciated, the offending bony

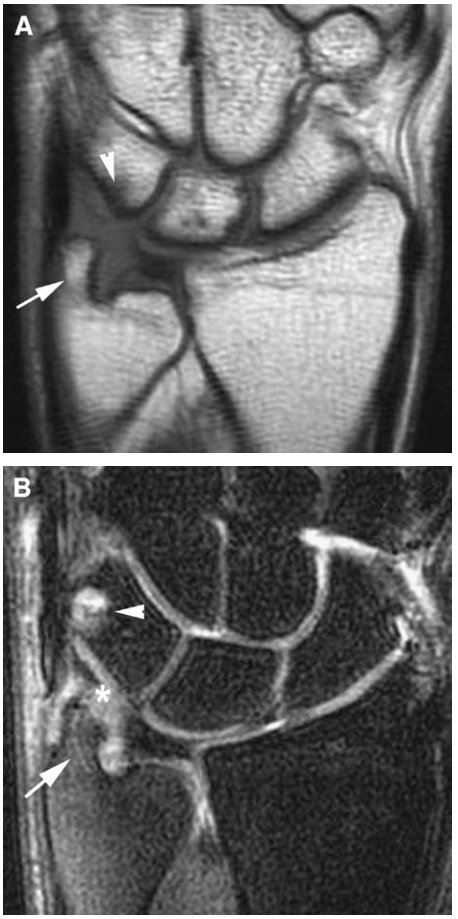

Fig. 11. US impaction syndrome in a 44-year-old man with severe chronic ulnar-sided pain. Coronal T1-weighted MR image (*A*) shows an excessively long ulnar styloid (US) process (*arrow*), focal subchondral sclerosis on the proximal aspect of the triquetrum (*arrowhead*). Coronal fat-suppressed T2-weighted (*B*) MR image shows chondromalacia of the triquetral bone and tip of the US with extensive subchondral edema (*arrow*), and small subchondral cysts in the triquetrum (*arrowhead*). Note ulnar-sided wrist synovitis (*asterisk*). Resection of the two most distal millimeters of the US process was performed, resulting in good recovery of function and relief of symptoms.

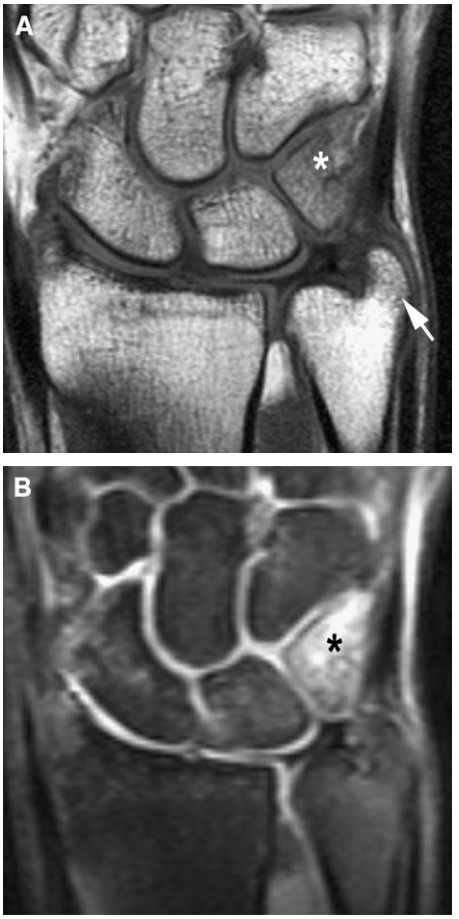

Fig. 12. Ulnar styloid (US) impaction syndrome in a 32-year-old man with chronic ulnar-sided pain without history of trauma. Coronal T1-weighted (*A*) MR image reveals US with a parrot beaked appearance (*arrow*) and diffuse bone marrow edema within the triquetral bone (*asterisk*). Corresponding coronal fat-suppressed T2-weighted (*B*) MR image shows extensive subchondral edema within the triquetral bone (*asterisk*). Partial ulnar styloidectomy was performed, resulting in complete resolution of symptoms.

fragment should be removed (if possible by arthroscopy) and range of motion immediately started.

Hamatolunate impaction syndrome

Hamatolunate impaction is an uncommon cause of ulnar-sided wrist pain secondary to chondromalacia of the proximal pole of the hamate bone in patients with lunate bones that have a medial articular facet on the distal surface for articulation with the hamate bone (Fig. 15) [71–74].

The anatomic variation of an articulation between the hamate and the lunate described by Viegas et al [71] (type II lunate bone), which is present in between 57% and 73% of wrists, produces alteration of the normal uniform loading and focally altered mechanics that leads to a higher incidence of cartilage erosion with

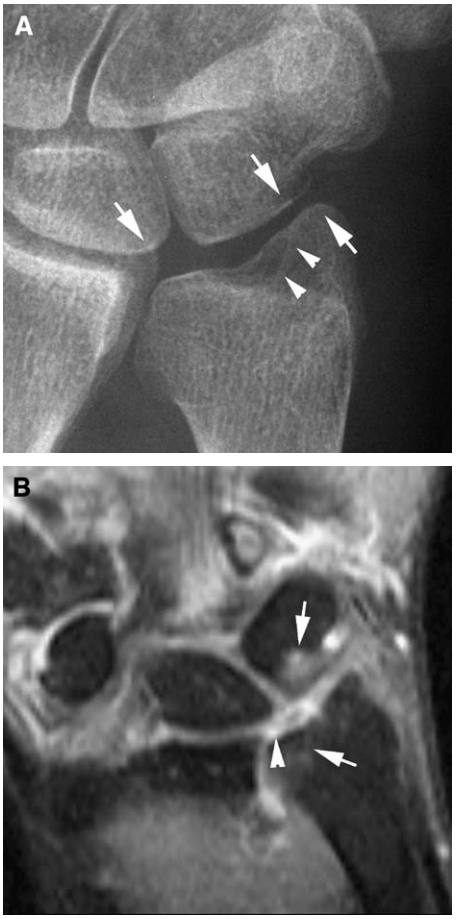

Fig. 13. Ulnar styloid (US) impaction syndrome in a 38-year-old woman with chronic ulnar-sided pain and enlarged US process. Posteroanterior radiograph (*A*) shows an enlarged US process with a broad base and obliteration of the ulnar fovea. Note subtle interface into the US (*arrowheads*) that suggests bone apposition, perhaps secondary to old traumatic event. Significant reduction of ulnocarpal space and slight subchondral sclerosis in the ulnar pole, lunate, triquetrum and US (*arrows*) can also be seen. Coronal fat-suppressed T2-weighted (*B*) MR image shows chondromalacia of the triquetral, lunate, ulnar head and US, with secondary subchondral edema (*arrows*). Note central perforation of the triangular fibrocartilage (TFC) (*arrowhead*). Arthroscopic US remodelling was performed with good results.

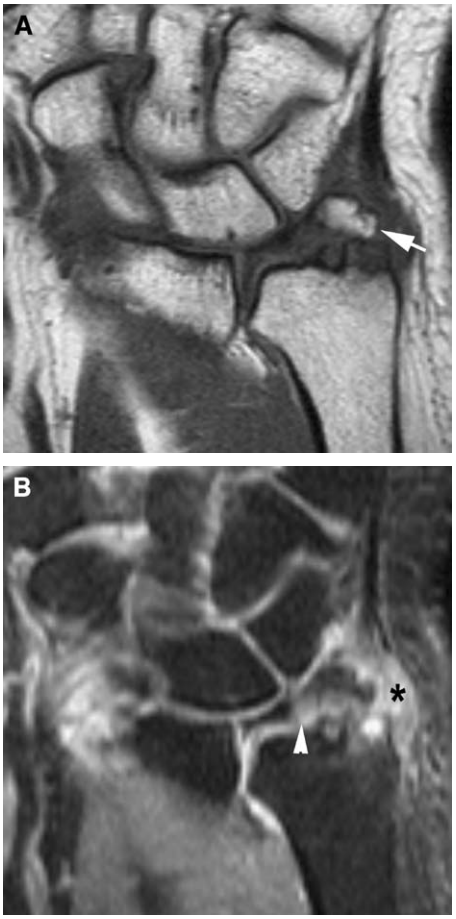

Fig. 14. Ulnar styloid (US) impaction syndrome secondary to type II nonunion of the US process in a 33-year-old man with insidious ulnar-sided pain. Coronal T1-weighted (*A*) and fat-suppressed T2-weighted (*B*) MR images reveal nonunion of the US process (*arrow*) associated with ulnar avulsion of the triangular fibrocartilage (TFC) complex (Palmer class IB TFC complex injury) (*arrowhead in B*), ulnar wrist synovitis and tenosynovitis of the ECU (*asterisk*). Results of arthroscopic examination revealed early focal chondromalacia of the triquetral bone, not seen in MR imaging examination. The patient underwent excision of the fragment and repair of the TFC complex, with excellent results.

exposed subchondral bone on the proximal pole of the hamate bone than in those without this articulation (type I lunate bone) [71–75].

The repeated impingement and abrasion of these two bones when the wrist is used in full ulnar deviation is the suggested mechanism for the development of the chondromalacia [74,76,77].

Patients experience pain in full ulnar deviation of the wrist and it is by repeating this maneuver, especially when combined with first holding the distal carpal row in forced supination, that their pain can be reproduced [74].

The hamatolunate articulation is seen frequently during arthroscopy of the midcarpal joint,

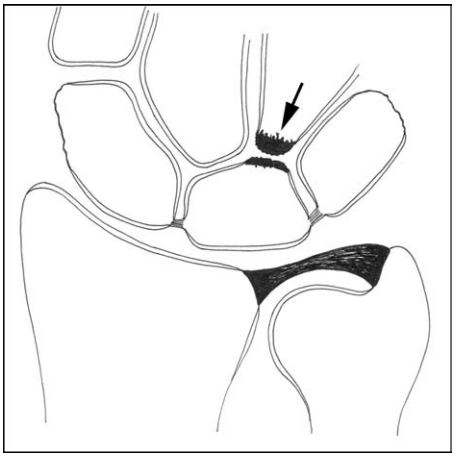

Fig. 15. Diagram illustrates hamatolunate impaction syndrome, with Viegas type II lunate bone, chondromalacia of the proximal pole of the hamate bone and secondary subchondral changes (*arrow*).

but only about 40% of those articulations are evident radiologically. This facet is variable in size (from 1.2 to 12 mm) and may occupy between 10% and 50% of the distal aspect of the lunate [71,72,78]. In the clinical setting of ulnar-sided wrist pain, the radiographic evidence of a type II lunate bone should raise the question of arthrosis at the proximal pole of the hamate as the most likely source of the complaint.

MR imaging has low sensitivity for early stages of chondromalacia, but can detect bone edema, sclerosis, and subchondral cysts in the proximal pole of the hamate bone as secondary signs of chondromalacia and focal osteoarthritis (Fig. 16) [8,18,78].

Arthroscopic burring of the apex of the hamate bone through a midcarpal portal represents the state-of-the-art treatment of this condition because it relieves symptoms and does not adversely affect carpal mechanics [4,74].

Fig. 16. Hamatolunate impaction syndrome in a 31-year-old man. Coronal T1-weighted (*A*) and fat-suppressed T2-weighted (*B*) MR images show type II lunate bone with advanced chondromalacia in the proximal pole of the hamate bone, secondary subchondral sclerosis (*arrow*) and bone marrow edema (*asterisk*). Arthroscopic resection of the proximal pole of the hamate bone resulted in completely relief of symptoms.

Combined ulnar and US impaction syndrome

We have recently recognized a new type of ulnar impaction, which we have named ulnar and US impaction syndrome or double ulnar impaction syndrome. This is a combined collision between the ulnar head and the US against the carpus (Fig. 17) (Francisco del Piñal, unpublished data, 2002).

Posttraumatic shortening of the distal radius after a distal radius fracture combined with dorsal malalignment leads to a positive ulnar variance, one of the major causes of ulnar impaction syndrome [79,80]. In this scenario a previously asymptomatic, marginally long, or beaked US will become longer and produce concomitant impaction of the US onto the proximal aspect of the triquetral bone and the ulnar-side pole of the lunate bone (Fig. 18). A chip fracture of the US that heals in an elongated position will produce similar symptoms.

Less frequently this entity may occur in patients with positive ulnar variance and elongated or radially deviated US (Fig. 19). The symptom complex that frequently accompanies this entity

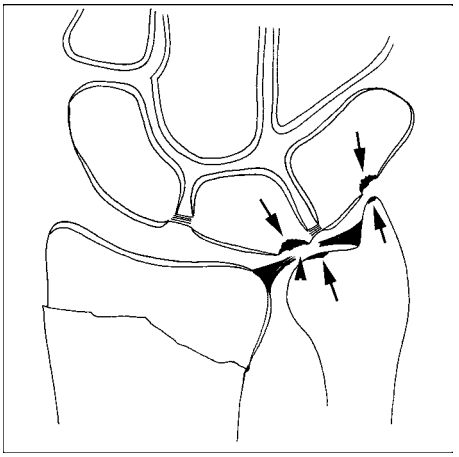

Fig. 17. Coronal diagram illustrates the full spectrum of pathologic conditions in combined ulnar and US impaction syndromes, including chondromalacia and secondary subchondral changes of the ulnar head, the ulnar side of the lunate bone, US process, and the triquetral bone (*arrows*), and central perforation of the triangular fibrocartilage (TFC) (*arrowhead*).

includes nonspecific wrist pain, loss of motion, and weakness.

Standardized AP and lateral radiographs are helpful in the evaluation of radial deformity, subluxation, ulnar variance, and US morphological variations or pathological conditions. Five measurements can be used to evaluate the distal end of the radius: radial inclination, radial length, ulnar variance, radial tilt, and radial shift [41,79]. The US architecture measurements (US length, angle, and width) also should be recorded [60].

In addition to a positive ulnar variance and elongated or radially deviated US, characteristic radiographic findings in combined ulnar and US syndrome are sclerosis, osteopenia, and cysts formation in the distal ulna, in the proximal portion of the ulnar-sided lunate, tip of the US, and proximal aspect of the triquetrum. These changes, however, most often represent a chronic long-standing process, so findings on radiographs are often negative in the early course of the disease [8,56].

MR imaging can earlier detect the combined characteristic findings of these two impaction syndromes: bone marrow edema, subchondral sclerosis, and cysts in specific anatomic locations previously described as well as TFC complex and soft tissue lesions (see Figs. 18 and 19).

Taking into account that in most cases this is a secondary impaction syndrome, the choice of

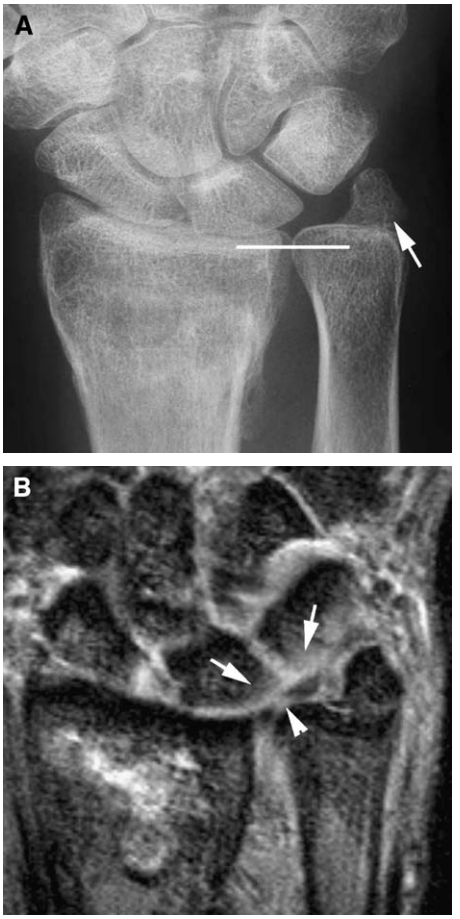

Fig. 18. Combined ulnar and ulnar styloid (US) impaction syndrome in a 58-year-old man with malunion of the distal radius fracture with radial shortening and elongated US. Posteroanterior radiograph (*A*) shows shortening distal radius, positive ulnar variance and elongated US (*arrow*). Coronal T2*-weighted (*B*) MR image reveals triangular fibrocartilage (TFC) central perforation, and subtle chondromalacia in the lunate and triquetrum. Arthroscopic examination confirmed TFC perforation and chondromalacia in the proximal ulnar carpus. Ulnar shortening osteotomy was performed with good recovery of function and relief of symptoms.

the procedure is dictated by the degree on radial malunion. When the radial malunion is severe (more than 10 degrees in the sagittal or frontal planes), the surgeon should try to restore the wrist joint anatomy by osteotomizing the distal radius, repositioning it, and interposing a bone graft into the defect created in the metaphyseal area: this will restore the radius to its position and length,

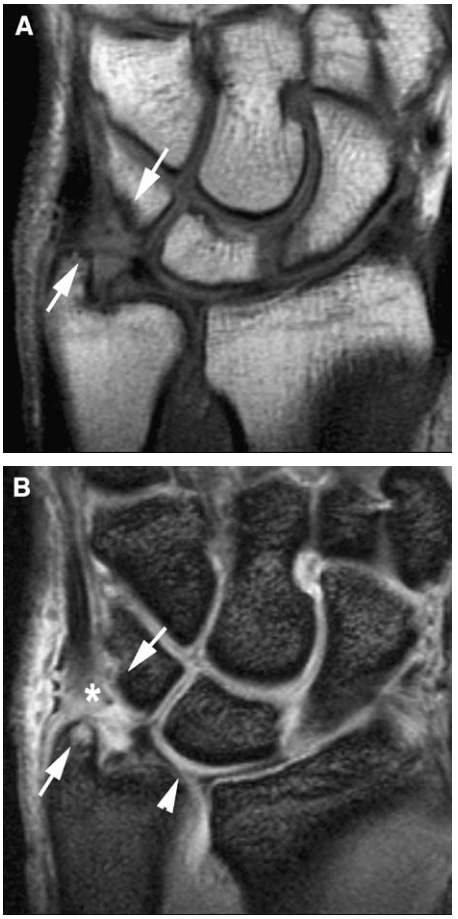

Fig. 19. Combined ulnar and ulnar styloid (US) impaction syndrome in a 37-year-old man with congenital ulnar positive variance and radially deviated or parrot-beaked US. Coronal T1-weighted (*A*) MR image shows subchondral sclerosis secondary to advanced chondromalacia in the tip of the US and in the dorsal aspect of the triquetrum (*arrows*). Corresponding coronal T2*-weighted (*B*) MR image shows advanced chondromalacia with secondary subchondral changes of the US (*arrow*) and triquetral bone (*arrows*). Note central triangular fibrocartilage (TFC) perforation (*arrowhead*) and ulnar wrist synovitis (*asterisk*). Arthroscopic debridement and partial ulnar styloidectomy were performed, with excellent results.

and the ulnar impaction will be corrected [79,81,82].

When the radial malunion is limited to shortening, but the sagital and frontal alignment is preserved (less than 10 degrees of deformity), the surgeon can restore DRUJ anatomy and physiological tension of the ulnocarpal ligaments by the much simpler shortening osteotomy of the ulna [82].

Restoration of the radius-ulna relationships, no matter how, will separate the ulnar dome and the ulna styloid from the carpus, correcting this double impingement.

In the authors' opinion, there is no role for the wafer procedure (open or arthroscopic) in combination with a styloid resection for this entity as neither will restore the ulnar head to its anatomic seat or tighten the ulnocarpal ligaments as the radial osteotomy or ulnar shortening will.

Finally, if irreparable damage to the sigmoid fossa has occurred during the fracture event, or degeneration of the ulnar head has taken place, the surgeon should consider the case as beyond repair and select any of the salvage procures available: Darrach, Sauve-Kapandji, or ulnar head prostheses [49–51].

Summary

MR imaging is an excellent modality for visualizing the full spectrum of abnormalities in ulnar-sided wrist impaction syndromes. Confirmation of clinical and conventional radiographic findings with MR imaging is often necessary to exclude other entities with similar clinical manifestations.

MR imaging allows earlier detection of an abnormality in the TFC complex, cartilage, or bone marrow of carpal bones and is helpful in formulating the extensive differential diagnosis in patients with ulnar wrist pain and limitation of motion. MR imaging is especially useful in planning surgical treatment by showing the exact location and extent of these lesions.

References

[1] Garcia-Elias M. Soft-tissue anatomy and relationships about the distal ulna. Hand Clin 1998;14(2):165–76.

[2] Loftus JB, Palmer AK. Disorders of the distal radioulnar joint and triangular fibrocartilage complex: an overview. In: Lichtman DM, Alexander AH, editors. The wrist and its disorders. Second edition. Philadelphia: WB Saunders; 1997. p. 385–414.

[3] Bowers WH. The distal radioulnar joint. In: Green DP, Hotchkiss RN, Pederson WC, Lampert R, editors. Green's operative hand surgery. Fourth edition. New York: Churchill Livingstone; 1999. p. 986–1032.

[4] Dailey SW, Palmer AK. The role of arthroscopy in the evaluation and treatment of triangular fibrocartilage complex injuries in athletes. Hand Clin 2000;16(3):461–76.
[5] Palmer AK, Werner FW. The triangular fibrocartilage complex of the wrist—anatomy and function. J Hand Surg 1981;6(2):153–62.
[6] Palmer AK. The distal radioulnar joint. Anatomy, biomechanics, and triangular fibrocartilage complex abnormalities. Hand Clin 1987;3(1):31–40.
[7] Viegas SF. Ulnar-sided wrist pain and instability. Instr Course Lect 1998;47:215–8.
[8] Cerezal L, del Pinal F, Abascal F, Garcia-Valtuille R, Pereda T, Canga A. Imaging findings in ulnar-sided wrist impaction syndromes. Radiographics 2002;22(1):105–21.
[9] Palmer AK, Werner FW. Biomechanics of the distal radioulnar joint. Clin Orthop 1984;187:26–35.
[10] Hulten O. Über anatomische variationen der handgelenkknochen. Acta Radiol 1928;155–69.
[11] Werner FW, Palmer AK, Fortino MD, Short WH. Force transmission through the distal ulna: effect of ulnar variance, lunate fossa angulation, and radial and palmar tilt of the distal radius. J Hand Surg 1992;17(3):423–8.
[12] Epner RA, Bowers WH, Guilford WB. Ulnar variance—the effect of wrist positioning and roentgen filming technique. J Hand Surg 1982;7(3): 298–305.
[13] Friedman SL, Palmer AK, Short WH, Levinsohn EM, Halperin LS. The change in ulnar variance with grip. J Hand Surg 1993;18(4):713–6.
[14] Tomaino MM. The importance of the pronated grip x-ray view in evaluating ulnar variance. J Hand Surg 2000;25(2):352–7.
[15] Garcia-Elias M. Kinetic analysis of carpal stability during grip. Hand Clin 1997;13(1):151–8.
[16] Escobedo EM, Bergman AG, Hunter JC. MR imaging of ulnar impaction. Skeletal Radiol 1995; 24(2):85–90.
[17] Palmer AK, Glisson RR, Werner FW. Ulnar variance determination. J Hand Surg 1982;7(4): 376–9.
[18] Mellado JM, Calmet J, Domenech S, Sauri A. Clinically significant skeletal variations of the shoulder and the wrist: role of MR imaging. Eur Radiol 2003;13(7):1735–43.
[19] Friedman SL, Palmer AK. The ulnar impaction syndrome. Hand Clin 1991;7(2):295–310.
[20] Imaeda T, Nakamura R, Shionoya K, Makino N. Ulnar impaction syndrome: MR imaging findings. Radiology 1996;201(2):495–500.
[21] Hodge JC, Yin Y, Gilula LA. Miscellaneous conditions of the wrist. In: Gilula LA, Yin Y, editors. Imaging of the wrist and hand. Philadelphia: Saunders; 1996. p. 523–46.
[22] Palmer AK. Triangular fibrocartilage complex lesions: a classification. J Hand Surg 1989;14(4): 594–606.
[23] Tomaino MM. Ulnar impaction syndrome in the ulnar negative and neutral wrist. Diagnosis and pathoanatomy. J Hand Surg 1998;23(6):754–7.
[24] Tomaino MM. Results of the wafer procedure for ulnar impaction syndrome in the ulnar negative and neutral wrist. J Hand Surg 1999;24(6):671–5.
[25] Tomaino MM, Weiser RW. Combined arthroscopic TFCC debridement and wafer resection of the distal ulna in wrists with triangular fibrocartilage complex tears and positive ulnar variance. J Hand Surg 2001; 26(6):1047–52.
[26] Nakamura R, Horii E, Imaeda T, Nakao E, Kato H, Watanabe K. The ulnocarpal stress test in the diagnosis of ulnar-sided wrist pain. J Hand Surg 1997;22(6):719–23.
[27] Stoller DW, Brody GA. The wrist and hand. In: Stoller DW, editor. Magnetic resonance imaging in orthopaedics and sports medicine. 2nd edition. Philadelphia: Lippincott-Raven; 1997. p. 851–993.
[28] Oneson SR, Scales LM, Timins ME, Erickson SJ, Chamoy L. MR imaging interpretation of the Palmer classification of triangular fibrocartilage complex lesions. Radiographics 1996;16(1):97–106.
[29] Oneson SR, Timins ME, Scales LM, Erickson SJ, Chamoy L. MR imaging diagnosis of triangular fibrocartilage pathology with arthroscopic correlation. AJR Am J Roentgenol 1997;168(6):1513–8.
[30] Sofka CM, Potter HG. Magnetic resonance imaging of the wrist. Semin Musculoskelet Radiol 2001; 5(3):217–26.
[31] Smith DK. Scapholunate interosseous ligament of the wrist: MR appearances in asymptomatic volunteers and arthrographically normal wrists. Radiology 1994;192(1):217–21.
[32] Loftus JB. Arthroscopic wafer for ulnar impaction syndrome. Tech Hand Upper Extrem Surg 2000;4: 182–8.
[33] Feldon P, Terrono AL, Belsky MR. The "wafer" procedure. Partial distal ulnar resection. Clin Orthop 1992;275:124–9.
[34] Tolat AR, Sanderson PL, De Smet L, Stanley JK. The gymnast's wrist: acquired positive ulnar variance following chronic epiphyseal injury. J Hand Surg 1992;17(6):678–81.
[35] Sagerman SD, Zogby RG, Palmer AK, Werner FW, Fortino MD. Relative articular inclination of the distal radioulnar joint: a radiographic study. J Hand Surg 1995;20(4):597–601.
[36] Tolat AR, Stanley JK, Trail IA. A cadaveric study of the anatomy and stability of the distal radioulnar joint in the coronal and transverse planes. J Hand Surg 1996;21(5):587–94.
[37] Deshmukh SC, Shanahan D, Coulthard D. Distal radioulnar joint incongruity after shortening of the ulna. J Hand Surg 2000;25(5):434–8.
[38] Constantine KJ, Tomaino MM, Herndon JH, Sotereanos DG. Comparison of ulnar shortening osteotomy and the wafer resection procedure as

treatment for ulnar impaction syndrome. J Hand Surg 2000;25(1):55–60.
[39] Shin AY, Weinstein LP, Berger RA, Bishop AT. Treatment of isolated injuries of the lunotriquetral ligament. A comparison of arthrodesis, ligament reconstruction and ligament repair. J Bone Joint Surg [Br] 2001;83(7):1023–8.
[40] Hotchkiss RN. Injuries to the interosseous ligament of the forearm. Hand Clin 1994;10(3):391–8.
[41] Graham TJ, Fischer TJ, Hotchkiss RN, Kleinman WB. Disorders of the forearm axis. Hand Clin 1998; 14(2):305–16.
[42] Bell MJ, Hill RJ, McMurtry RY. Ulnar impingement syndrome. J Bone Joint Surg [Br] 1985;67(1): 126–9.
[43] McKee MD, Richards RR. Dynamic radio-ulnar convergence after the Darrach procedure. J Bone Joint Surg [Br] 1996;78(3):413–8.
[44] Lees VC, Scheker LR. The radiological demonstration of dynamic ulnar impingement. J Hand Surg 1997;22(4):448–50.
[45] Wolfe SW, Mih AD, Hotchkiss RN, Culp RW, Keifhaber TR, Nagle DJ. Wide excision of the distal ulna: a multicenter case study. J Hand Surg 1998;23(2):222–8.
[46] Tsai TM, Stilwell JH. Repair of chronic subluxation of the distal radioulnar joint (ulnar dorsal) using flexor carpi ulnaris tendon. J Hand Surg 1984;9(3): 289–94.
[47] Jupiter JB, Masem M. Reconstruction of post-traumatic deformity of the distal radius and ulna. Hand Clin 1988;4(3):377–90.
[48] Sotereanos DG, Gobel F, Vardakas DG, Sarris I. An allograft salvage technique for failure of the Darrach procedure: a report of four cases. J Hand Surg 2002;27(4):317–21.
[49] Van Schoonhoven J, Fernandez DL, Bowers WH, Herbert TJ. Salvage of failed resection arthroplasties of the distal radioulnar joint using a new ulnar head prosthesis. J Hand Surg 2000;25(3):438–46.
[50] Scheker LR. Distal radioulnar prostheses to rescue the so-called salvage procedure. In: Simmen BR, Allieu Y, Lluch A, Stanley J, editors. Hand arthroplasties. London: Dunitz; 2000. p. 151–8.
[51] Scheker LR, Babb BA, Killion PE. Distal ulnar prosthetic replacement. Orthop Clin North Am 2001;32(2):365–76.
[52] De Smet L, Peeters T. Salvage of failed Sauve-Kapandji procedure with an ulnar head prosthesis: report of three cases. J Hand Surg 2003;28(3): 271–3.
[53] Horii E, Nakamura R, Nakao E, Kato H, Yajima H. Distraction lengthening of the forearm for congenital and developmental problems. J Hand Surg 2000;25(1):15–21.
[54] Scheker LR, Severo A. Ulnar shortening for the treatment of early post-traumatic osteoarthritis at the distal radioulnar joint. J Hand Surg 2001;26(1): 41–4.
[55] Fernandez DL, Capo JT, Gonzalez E. Corrective osteotomy for symptomatic increased ulnar tilt of the distal end of the radius. J Hand Surg 2001;26(4): 722–32.
[56] Tomaino MM, Gainer M, Towers JD. Carpal impaction with the ulnar styloid process: treatment with partial styloid resection. J Hand Surg 2001; 26(3):252–5.
[57] Biyani A, Mehara A, Bhan S. Morphological variations of the ulnar styloid process. J Hand Surg 1990;15(3):352–4.
[58] Timins ME. The wrist and the hand: MRI. In: Shirkhoda A, editor. Variants and pitfalls in body imaging. Philadelphia: Lippincott, Williams & Wilkins; 2000. p. 585–615.
[59] Yanagida H, Ishii S, Short WH, Werner FW, Weiner MM, Masaoka S. Radiologic evaluation of the ulnar styloid. J Hand Surg 2002;27(1):49–56.
[60] Garcia-Elias M. Dorsal fractures of the triquetrum-avulsion or compression fractures? J Hand Surg 1987;12(2):266–8.
[61] Topper SM, Wood MB, Ruby LK. Ulnar styloid impaction syndrome. J Hand Surg 1997;22(4): 699–704.
[62] Levy M, Fischel RE, Stern GM, Goldberg I. Chip fractures of the os triquetrum: the mechanism of injury. J Bone Joint Surg [Br] 1979;61(3):355–7.
[63] Kikuchi Y, Nakamura T. Avulsion fracture at the fovea of the ulna. A report of two cases. J Hand Surg 1998;23(2):176–8.
[64] Bacorn RW, Kurtzke JF. Colles' fracture: a study of two thousand cases from the New York State Workmen's Compensation Board. J Bone Joint Surg [Am] 1953;35:643–58.
[65] Cooney WP, Dobyns JH, Linscheid RL. Complications of Colles' fractures. J Bone Joint Surg [Am] 1980;62:613–9.
[66] Hauck RM, Skahen J III, Palmer AK. Classification and treatment of ulnar styloid nonunion. J Hand Surg 1996;21(3):418–22.
[67] Lindau T, Adlercreutz C, Aspenberg P. Peripheral tears of the triangular fibrocartilage complex cause distal radioulnar joint instability after distal radial fractures. J Hand Surg 2000;25(3):464–8.
[68] May MM, Lawton JN, Blazar PE. Ulnar styloid fractures associated with distal radius fractures: incidence and implications for distal radioulnar joint instability. J Hand Surg 2002;27(6):965–71.
[69] Minami A, Ishikawa J, Kondo E. Painful unfused separate ossification center of the ulnar styloid: a case report. J Hand Surg 1994;19(6):1045–7.
[70] Hermansdorfer JD, Kleinman WB. Management of chronic peripheral tears of the triangular fibrocartilage complex. J Hand Surg 1991;16(2):340–6.
[71] Viegas SF, Wagner K, Patterson R, Peterson P. Medial (hamate) facet of the lunate. J Hand Surg 1990;15(4):564–71.
[72] Viegas SF, Patterson RM, Hokanson JA, Davis J. Wrist anatomy: incidence, distribution, and corre-

lation of anatomic variations, tears, and arthrosis. J Hand Surg 1993;18(3):463–75.
[73] Viegas SF. Variations in the skeletal morphologic features of the wrist. Clin Orthop 2001;383:21–31.
[74] Thurston AJ, Stanley JK. Hamato-lunate impingement: an uncommon cause of ulnar-sided wrist pain. Arthroscopy 2000;16(5):540–4.
[75] Sagerman SD, Hauck RM, Palmer AK. Lunate morphology: can it be predicted with routine x-ray films? J Hand Surg 1995;20(1):38–41.
[76] Nakamura K, Beppu M, Patterson RM, Hanson CA, Hume PJ, Viegas SF. Motion analysis in two dimensions of radial-ulnar deviation of type I versus type II lunates. J Hand Surg 2000;25(5): 877–88.
[77] Viegas SF, Tencer AF, Cantrell J, Chang M, Clegg P, Hicks C, et al. Load transfer characteristics of the wrist. Part I. The normal joint. J Hand Surg 1987;12(6):971–8.
[78] Malik AM, Schweitzer ME, Culp RW, Osterman LA, Manton G. MR imaging of the type II lunate bone: frequency, extent, and associated findings. AJR Am J Roentgenol 1999;173(2):335–8.
[79] Jupiter JB, Fernandez DL. Complications following distal radial fractures. Instr Course Lect 2002;51: 203–19.
[80] Steinborn M, Schurmann M, Staebler A, Wizgall I, Pellengahr C, Heuck A, et al. MR imaging of ulnocarpal impaction after fracture of the distal radius. AJR Am J Roentgenol 2003;181(1): 195–8.
[81] Prommersberger KJ, Van Schoonhoven J, Lanz UB. Outcome after corrective osteotomy for malunited fractures of the distal end of the radius. J Hand Surg 2002;27(1):55–60.
[82] Fernandez DL. Reconstructive procedures for malunion and traumatic arthritis. Orthop Clin North Am 1993;24(2):341–63.